Janisse, J. J., Lee, J., & Chugani, H. T. Developmental changes in brain serotonin synthesis capacity in autistic and nonautistic children. *Annals of neurology*, 45 (1999) 287-95.

13) Durston, S., Davidson, M. C., Tottenham, N., Galvan, A., Spicer, J., Fossella, J. A., & Casey, B. J. A shift from diffuse to focal cortical activity with development. *Developmental Sciences* , 9, (2006) 1-20.

14) Buckner, R. L., Andrews-Hanna, J. R., & Schagter, D. L. The brain's default network. Anatomy, function, and relevance to disease. *Annals of the New York Academy of Sciences*, 1124, (2008) 1-38.

15) 外林大作, 千葉ロール・プレイング研究会 (1981). 教育の現場におけるロール・プレイングの手引 誠信書房

16) 冨田博之 (1974). 現代演劇教育論 日本演劇教育連盟

17) Sakatani, K., Yamashita, D., Yamanaka, T., Oda, M., Yamashita, Y., Hoshino, T., Fujiwara, N. Murata,Y., & Katayama, Y. Changes of cerebral blood oxygenation and optical pathlength during activation and deactivation in the prefrontal cortex measured by time-resolved near infrared spectroscopy. *Life Sciences*, 78, (2006) 2734 -2741.

18) Castaneda, A., McCandless, B. R., & Palermo, D.S. The Children's Form of the Manifest Anxiety Scale. *Child Development*, 27, (1956) 317-326.

19) Baas, D., Aleman, A., Kahn, & Kahn, R. S. Lateralization of amygdala activation: a systematic review of functional neuroimaging studies. *Brain research. Brain research reviews*, 45, (2004) 96-103.

20) Fallgatter, A. J., Muller, T. J., & Strik, W. K. Prefrontal hypooxygenation during language processing assessed with near-infrared spectroscopy. *Neuropsychobiology*, 37, (1998)215-218.

21) Kuwabata, H., Kasai, K., Takizawa,R., Kawakubo, Y., Yamasue, H., Rogers, M. A., Ishijima, M ., Watanabe, K., & Kato,N. Decreased prefrontal activation during letter fluency task in adults with pervasive developmental disorders : a near-infrared spectroscopy study. *Behavioural brain research*, 172, (2006) 272-277.

22) Davidson, R.J., & Irwin, W. The functional neuroanatomy of emotion and affective style. *Trends in Cognive Sciences*, 3, (1999) 11-21.

23) Fischer, H., Andersson, J.L., Furmark, T., Wik, G., & Fredrikson, M. Right-sided human prefrontal brain activation during acquisition *of conditioned fear. Emotion* , 2, (2002) 233-241.

24) 伊藤宏樹・平山正昭・古池保雄 神経不全症患者の起立性低血圧時脳血流自動調節能—近赤外線分光法による検討— 臨床脳波, 47, (2005) 629-632.

昨日から今日のあなた自身について，はい か いいえ に　○をつけましょう.

1. 朝，すっきり起きられた（　はい　・　いいえ　）
2. 頭がいたくなった，いたい（　はい　・　いいえ　）
3. おなかがいたくなった，いたい（　はい　・　いいえ　）
4. 元気だ（　はい　・　いいえ　）
5. 肩こりがあった，ある（　はい　・　いいえ　）
6. 食欲がでなかった，ない（　はい　・　いいえ　）
7. 体がだるくなった，だるい（　はい　・　いいえ　）
8. 昼間でもねむかった，ねむい（　はい　・　いいえ　）
9. ご飯がおいしく食べられた（　はい　・　いいえ　）
10. 夜，なかなかねむれなかった（　はい　・　いいえ　）
11. 自分は人の役に立っていると思う（　はい　・　いいえ　）
12. わたしなんかいないほうがよいと思う（　はい　・　いいえ　）
13. やればできると思う（　はい　・　いいえ　）
14. イライラする（　はい　・　いいえ　）
15. やる気がしない（　はい　・　いいえ　）
16. 学校は楽しいと思う（　はい　・　いいえ　）
17. 人と話すのはいやだ（　はい　・　いいえ　）
18. 家は楽しいと思う（　はい　・　いいえ　）
19. 困ったことや心配なことを話せる人がいる（　はい　・　いいえ　）
20. 自分のことが好きだ（　はい　・　いいえ　）

巻末参考資料

実験2で用いた不定愁訴に関する質問項目を示す.

採点は，2, 3, 5, 6, 7, 8, 10, 14, 15, 17については，はいを1点，いいえを0点とし，1, 4, 9, 11, 12, 13, 16, 18, 19, 20については，はいを0点，いいえを1点として，全問の合計得点を出した.

Journal of Neuroscience Research

Journal of Neuroscience Research 88:2911–2922 (2010)

Analysis of Gene Expression Changes Associated With Long-Lasting Synaptic Enhancement in Hippocampal Slice Cultures After Repetitive Exposures to Glutamate

**Katsuhiro Kawaai,[1] Keiko Tominaga-Yoshino,[2] Tomoyoshi Urakubo,[2] Naoko Taniguchi,[2] Yasumitsu Kondoh,[3] Hideo Tashiro,[3] Akihiko Ogura,[2] and Tomoko Tashiro[1]*

[1]Department of Chemistry and Biological Science, School of Science and Engineering, Aoyama Gakuin University, Kanagawa, Japan
[2]Osaka University Graduate School of Frontier Biosciences and Osaka University Graduate School of Science, Osaka, Japan
[3]Probing Technology Laboratory, Discovery Research Institute, RIKEN, Wako, Saitama, Japan

We have previously shown that repetitive exposures to glutamate (100 μM, 3 min, three times at 24-hr intervals) induced a long-lasting synaptic enhancement accompanied by synaptogenesis in rat hippocampal slice cultures, a phenomenon termed *RISE* (for repetitive LTP-induced synaptic enhancement). To investigate the molecular mechanisms underlying RISE, we first analyzed the time course of gene expression changes between 4 hr and 12 days after repetitive stimulation using an original oligonucleotide microarray: "synaptoarray." The results demonstrated that changes in the expression of synapse-related genes were induced in two time phases, an early phase of 24–96 hr and a late phase of 6–12 days after the third stimulation. Comprehensive screening at 48 hr after the third stimulation using commercially available high-density microarrays provided candidate genes responsible for RISE. From real-time PCR analysis of these and related genes, two categories of genes were identified, 1) genes previously reported to be induced by physiological as well as epileptic activity (*bdnf, grm5, rgs2, syt4, ania4/carp/dclk*) and 2) genes involved in cofilin-based regulation of actin filament dynamics (*ywhaz, ssh1l, pak4, limk1, cfl*). In the first category, synaptotagmin 4 showed a third stimulation-specific up-regulation also at the protein level. Five genes in the second category were coordinately up-regulated by the second stimulation, resulting in a decrease in cofilin phosphorylation and an enhancement of actin filament dynamics. In contrast, after the third stimulation, they were differentially regulated to increase cofilin phosphorylation and enhance actin polymerization, which may be a key step leading to the establishment of RISE.

Key words: long-term potentiation; long-lasting plasticity; synaptogenesis; DNA microarray; repetitive stimulation

We can discriminate at least two phases in memory, short-term memory, which endures for a few hours, and long-term memory, which persists for several days and often much longer (Bear et al., 2001). Short-lasting synaptic plasticity, the presumed cellular basis of short-term memory, is thought to be accomplished by the rapid modification of synaptic strength in existing synapses (Lisman et al., 2002; Collingridge et al., 2004), whereas long-lasting synaptic plasticity representing long-term memory is associated with gene expression, de novo protein synthesis, and formation of new synaptic connections (Steward and Schuman, 2001; Lynch, 2004). Consistent with this idea, protein synthesis inhibitors can block the late-phase of long-term potentiation

Additional Supporting Information may be found in the online version of this article.

Katsuhiro Kawaai's current address is Calcium Oscillation Project, International Cooperative Research Project—Solution Oriented Research for Science and Technology, Japan Science and Technology Agency, 2-1 Hirosawa, Wako, Saitama 351-0198, Japan

Contract grant sponsor: High-Tech Research Center Project for Private Universities; Contract grant number: 20310037 (to T.T.); Contract grant sponsor: Ministry of Education, Culture, Sports, Science and Technology (MEXT) of the Japanese Government; Contract grant number: 19300108 (to A.O.); Contract grant sponsor: Ministry of Health, Labour and Welfare of the Japanese Government (to T.T.).

*Correspondence to: Tomoko Tashiro, Department of Chemistry and Biological Science, School of Science and Engineering, Aoyama Gakuin University, 5-10-1 Fuchinobe, Chuo-ku, Sagamihara, Kanagawa 252-5258, Japan. E-mail: ttashiro@aoyamagakuin.jp

Received 17 February 2010; Revised 29 April 2010; Accepted 12 May 2010

Published online 21 June 2010 in Wiley Online Library (wileyonlinelibrary.com). DOI: 10.1002/jnr.22457

(L-LTP) but leave the early-phase LTP (E-LTP) unaffected (Otani et al., 1989; Frey et al., 1996). Although several studies have reported that synaptic activities modulated transcription (Klann and Dever, 2004), the molecular mechanism underlying the conversion from the short-lasting plasticity to the long-lasting one remains poorly understood, mainly because of the lack of good model systems that allow the prolonged examination of synapse formation.

With cultured rat hippocampal slices, we have previously shown that repetitive exposures to glutamate (100 μM, 3 min, three times at 24-hr intervals) or repetitive protein kinase A (PKA) activation (forskolin, 50 μM, 3 min, three times at 24-hr intervals) induced an enhancement of excitatory postsynaptic potential (EPSP) coupled with synaptogenesis that lasted for more than 3 weeks (Tominaga-Yoshino et al., 2002, 2008; Shinoda et al., 2003; Urakubo et al., 2006). Although similar glutamate exposure or PKA activation once or twice produced L-LTP accompanied by acute morphological changes, it lasted for less than 24 hr. We thus concluded that more than three repetitions of the stimulation for LTP at appropriate intervals (3–24 hr) was necessary for the conversion of short-lasting enhancement into a long-lasting one (i.e., lasting for weeks) coupled with synaptogenesis. To distinguish this repetitive L-LTP-induced synaptic enhancement from the conventional single LTP, we named this phenomenon *RISE* (repetitive LTP-induced synaptic enhancement) in previous reports (Tominaga-Yoshino et al., 2002, 2008). The RISE in cultured hippocampal slices provides us with a good model with which to investigate the molecular mechanisms of conversion from the short-lasting plasticity to the long-lasting one.

Various studies have shown that experimental stimuli inducing L-LTP were accompanied by de novo transcription and translation of genes related to synaptic plasticity (Otani et al., 1989; Frey et al., 1996; Lynch, 2004). Because RISE was accompanied by an increase in the number of morphologically identifiable synaptic sites, we first analyzed the time course of gene expression changes after repetitive stimulation to elucidate the essential time window of synaptogenesis involved in this phenomenon. For this purpose, we used our original microarray, "synaptoarray," focused on 295 genes involved mainly in synaptic structure and function (Takahashi et al., 2005), which was capable of monitoring synaptogenesis in the developing cerebellum in vivo (Takahashi et al., 2005) as well as synaptic activity-dependent gene expression changes accompanying tetrodotoxin application in cultured neurons (Kitamura et al., 2007). The results revealed that dynamic changes in gene expression induced by repetitive glutamate stimulation were composed of two time phases, an early phase of 24–96 hr and a late phase of 6–12 days after the last stimulation.

Given these results, we carried out a comprehensive screening with high-density arrays 48 hr after the third stimulation. With several candidate genes selected from microarray data and related genes, up-regulation by repetitive stimulation was confirmed by real-time PCR, resulting in the identification of pathways responsible for the development of long-lasting synaptic plasticity.

MATERIALS AND METHODS

Slice Culture of the Rat Hippocampus and Glutamate Treatment

Hippocampal slices from Wistar/ST rat pups at postnatal day 8 (Nihon SLC, Shizuoka, Japan) were cultured as described previously (Tominaga-Yoshino et al., 2008). Before we began the stimulation experiments, the cultures were maintained at 34°C in humidified air for 12 days with medium renewal twice per week, during which time the slices became stabilized both physically and physiologically (Muller et al., 1993; Gahwiler et al., 1997). All animal treatments have been approved by the animal experimentation committees of Aoyama Gakuin and Osaka Universities. They were carried out under veterinary supervision and in accordance with the *Guidelines for the use of animals in neuroscience research* (Society for Neuroscience, 1992). Glutamate-exposure to induce LTP was carried out following the protocol described previously (Tominaga-Yoshino et al., 2008). The glutamate solution for stimulation (Glu solution) contained 100 μM glutamate in K^+-elevated, Mg^{2+}-free, HEPES-buffered balanced salt solution (15K HBSS; composed of 120.4 mM NaCl, 15 mM KCl, 5.5 mM glucose, 3 mM $CaCl_2$, 10 mM Hepes-NaOH, pH 7.4). Mock stimulation solution was composed of HBSS with low KCl concentration (5K BSS; composed of 130 mM NaCl, 5.4 mM KCl, 5.5 mM glucose, 1.26 mM $CaCl_2$, 0.8 mM $MgCl_2$, 10 mM HEPES-NaOH, pH 7.4). Healthy slices (judged from opacity) were exposed to Glu solution or mock stimulation solution for 3 min at 34°C each time. As shown in Figure 1, glutamate exposure was repeated three times at 24-hr intervals starting on day 12 in vitro (DIV 12) for the three times glutamate-stimulated ([3G]) series. Slices for the twice-stimulated ([2G]) series were exposed first to mock stimulation solution and then twice to Glu solution at 24-hr intervals each. Control slices were exposed three times to mock stimulation solution. Thirty similarly treated slices were used at each time point for RNA extraction.

Histological Evaluation of Cell Viability

Apoptotic cells were distinguished from viable cells by the incorporation of propidium iodide (PI; Sigma, St. Louis, MO). At 24 hr after the third stimulation, PI (final 10 μg/ml) was added to hippocampal slice cultures and incubated for a further 24 hr at 34°C. Slices exposed to kainic acid (KA; 100 μM) in the presence of PI for 24 hr served as the positive control in this assay. Two CA1 regions per slice were photographed with identical incident light intensity and exposure time with a fluorescence microscope (IX-50; Olympus, Tokyo, Japan) at 48 hr after the third stimulation. PI fluorescence intensity was measured on each micrograph in NIH Image software (Tominaga-Yoshino et al., 2002) and normalized by the background fluorescence acquired in the region not occupied by the slice.

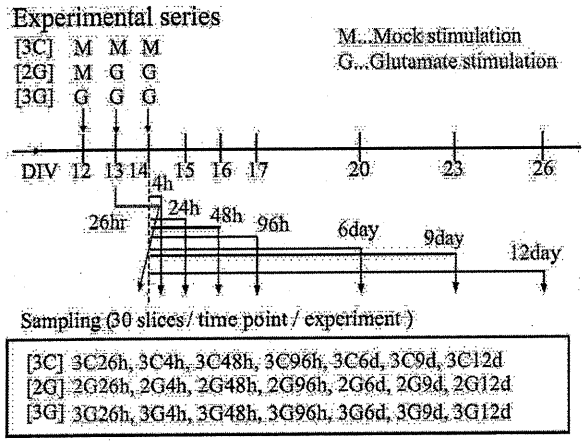

Fig. 1. Stimulation and sampling procedures. As described in Materials and Methods, hippocampal slices obtained from P8 rats were maintained in culture for 12d (DIV 12) before the start of the experiment to be stabilized both physically and physiologically. Slices were then stimulated in three ways ([3C], [2G], and [3G]) at 24-hr intervals on DIV12, 13, and 14. At each time point after the third stimulation, 30 each of the [3C], [2G], and [3G] slices were pooled (five slices × six wells) and used for RNA preparation. As a standard time point before the third stimulation, 26 hr after the second stimulation was used (26h). For protein extraction and Western blotting, 24 each of the slices stimulated in the three ways were pooled at 48 hr after the third stimulation.

Microarrays and Hybridization Conditions

Original oligonucleotide microarray was prepared as previously described (Takahashi et al., 2005). The contents of the synaptoarray are listed in Supporting Information Table I. A high-density microarray with oligonucleotide probes for 22,575 genes (rat oligoDNA microarray; Agilent Technologies, Palo Alto, CA) was used for screening genes differentially expressed by repetitive stimulation. Total RNA was prepared from pools of 30 similarly treated hippocampal slices using Trizol reagent (Invitrogen, Carlsbad, CA), reverse-transcribed with an oligo-dT primer containing the promoter sequence for T7 RNA polymerase, and amplified using RNA Transcript SureLABEL Core Kit (Takara Bio Inc., Shiga, Japan) with amino-allyl UTP incorporation. Amplified cRNA was purified with a QIAquick Nucleotide Removal Kit (Qiagen, Valencia, CA) and coupled either with cyanine 3 (Cy3; [3C] or [2G] slices) or with cyanine 5 (Cy5; [3G] slices). Labeled cRNA was purified with QIAquick Nucleotide Removal Kit (Qiagen) and fragmented using RNA Fragmentation Reagents (Ambion Diagnostics, Austin, TX). For one microarray, 1 μg each of Cy3- and Cy5-labeled samples to be compared was mixed in a final 500 μl of hybridization solution containing the following components at the following final concentrations; 0.02 μg/μl mouse Cot1-DNA (Invitrogen), 6 ng/μl oligo-dA 10mer (Sigma-Genosys, Hokkaidou, Japan), 0.3 μg/μl yeast tRNA (Invitrogen), 3.4× SSC, 0.3 ml/liter SDS (Gibco; 10 ml/liter SDS; DeRisi et al., 1996). The mixture was heated at 95°C for 1 min and clarified by centrifugation. Hybridization was performed in a hybridization chamber (Agilent Technologies) at 55°C for 16 hr with rotation (5 rpm). After hybridization, the chamber was disassembled in wash buffer I (6× SSC, 0.005 ml/liter Triton X-102), and the array slide was washed successively in wash buffer I for 10 min and wash buffer II (0.1× SSC, 0.005 ml/liter Triton X-102) for 5 min on ice and dried with N_2 gas.

Microarray Data Acquisition and Analysis

After hybridization, microarrays were scanned with DNAscope IV (GeneFocus Biomedical Photometrics Inc.). The fluorescence intensity signals from microarray images were quantified with ImaGene 5.5 (Biodiscovery, Los Angeles, CA) using the local background correction (GeneSight 3.5.2; Biodiscovery). The background-corrected Cy3 and Cy5 fluorescence intensity data from the synaptoarray were exported to Microsoft Excel and normalized using five internal standard genes (*rpL3, rpL13a, rpL22, rpL23, Ppia*) as described previously (Takahashi et al., 2005). Data from the high-density array were normalized by global normalization. Gene expression profiles were obtained from K-mean cluster analysis with software Gene Cluster (written by Michael Eisen, Stanford University).

Real-Time Quantitative Fluorescence-Based PCR

Expression levels of representative genes were quantified by fluorescence-based real-time PCR using the Smart Cycler System (Applied Cepheid) with Takara ExTaq (Takara Bio Inc.) and SYBR Green I (Molecular Probes, Eugene, OR) and were normalized with *rpl13a* as an internal standard. PCR primers (Table I) were designed in Oligo 6.0 primer analysis software (Molecular Biology Insights).

Western Blotting

Western blotting was performed as described previously (Kawaai et al., 2009). Briefly, PVDF membranes with proteins separated by SDS-PAGE were blocked with 5.0% skim milk in PBS containing 0.05% Tween-20 (PBST) for 1 hr and probed with the primary antibody for 1 hr at RT. The primary antibodies used were mouse anti-β-actin antibody (Sigma), rabbit anti-Syt4 antibody (IBL, Gunma, Japan), rabbit anti-mGluR5 antibody (Upstate, Lake Placid, NY), rabbit anti-BDNF antibody (N-20; Santa Cruz Biotechnology, Santa Cruz, CA), rabbit antiphospho-cofilin antibody (ab12866; Abcam, Tokyo, Japan), and rabbit anticofilin antibody (ab42824; Abcam). After being washed with PBST, the membranes were incubated with an appropriate HRP-conjugated secondary antibody, and signals were detected with Immobilon Western Detection Reagents (Millipore, Bedford, MA). A FujiFilm LAS4000 miniluminescent image analyzer was used to photograph the blots. Quantitative determination was performed with Multi Gauge (3.0; Fujifilm, Tokyo, Japan).

Immunostaining and Phalloidin Staining

Cultured hippocampal slices were washed once with PBS, fixed with 4.0% paraformaldehyde in PBS for 10 min, permeabilized with 1% Triton X-100 in PBS (PBS-Tx) for 5 min, and blocked with 1.0% skim milk with 1.0% normal goat serum (Vector Laboratories, Burlingame, CA) in PBS-Tx for 60 min at RT. Slices were then incubated with rabbit

TABLE I. Primers for Real-Time Quantitative PCR

	Forward	Reverse
bdnf	GGAGGCTAAGTGGAGCTGACATAC	GTGCTTCCGAGCCTTCCTTTAGG
syt4	AGTTTTGGATTCTGAAAGGGGATC	TTGTCTCCTGGGGAAGTCACAG
ania4	AACACTCCTTCATTACTTGCTTCC	AGTGGTTCCTTCTACAATGTTGAG
grm5	GCCCTCACTCCACCATCGCC	CTCTGCGTGTAATCTCTGATGATG
rgs2	GAAGTCCAGATGTGGTTCTGTTG	ATTCTTCACTTCTCAGGGCTGTC
ywhaz	CCATGCGGATCAAGCACAGCG	TAGCCGTCATCTCAAGTTATTTCC
slc6a12	GTGCTCCAGGAATCTGTTTGCC	AGCAGAGAGCAGCAAGTCCAAG
gabarapl2	TAGAGGGCTGAAGAGATGGCTC	AGGCAGGTAAGGGCATCAGATG
slc6a11	CCAAGGTCAAAGGCGACGGTAC	TTTACACGCAGGGAAGGAAGGC
cfl1	GCTGCCCTTTTCCTGCCAGAC	GGGATGGAGGGAAAAGGACGG
ssh11	CGACAGAAGGAGAAAGAACTGAG	GCTCATTTCGGATTTCCTTAGAAG
limk1	CATCTCTTCACTCTGCTTCAGTTG	CCTTGCCTCTTTCAGTCCTGGT
pak4	TGTGTCTCTATCTCAGCCTGGG	TAACTTGAGGGATTGGCGGCAG
casp3	CCCATAAGCCTCCTTATTGCAC	CACCACATGCTGTATTTACTTAG
rpl13a	GGAAGTACCAGGCAGTGACAGC	CTTGAGGACCTCTGTGAACTTGC

anti-Syt4 antibody (IBL) for 60 min at R.T. After three washes with PBS for 15 min in total, Alexa 488-conjugated goat anti-rabbit IgG (Invitrogen) was applied for 60 min at R.T. For phalloidin staining, Alexa 594-conjugated phalloidin (Invitrogen) was applied to fixed and permeabilized slices for 60 min at R.T. After being washed with PBS, the coverslips were mounted with Vectashield (Vector Laboratories) and observed under a Nikon E-600 microscope (Nikon, Tokyo, Japan) for immunostaining. For phalloidin staining, the Z-projection images (2-μm step size, 15 sections, maximum intensity projection by FV1000 software) were obtained by confocal fluorescence microscopy (FV1000; Olympus, Tokyo, Japan). Quantitative determination was performed in ImageJ software (v1.42q; NIH).

Electron Microscopy

To prevent the destruction of actin microfilaments (Maupin-Szamier and Pollard, 1978), the slice was prepared as described by Mbassa et al. (1988) and Dinno and Mugnaini (2000), with minor modifications. Hippocampal slice cultures were fixed with 2% paraformaldehyde (PF) and 1.5% glutaraldehyde (GA) in 0.1 M phosphate buffer (PB) for 12 hr at 4°C, followed by washing in 0.1 M PB (3 × 5 min). These slices were rinsed in 50 mM maleate buffer (MB) at pH 6.0 for 5 min and incubated with phalloidin (10 mg/ml; Sigma), 1% tannic acid (TAAB, Berkshire, United Kingdom), and 5% dimethylsulfoxide (DMSO) in 50 mM MB, pH 6.0. After being washed in MB (3 × 5 min), the slices were stained en bloc in the dark at 4°C for 2 hr with 1% uranyl acetate in MB and washed again in the buffer for 3 × 5 min. In the subsequent steps, slices were dehydrated in a graded series of ethanol and infiltrated with Quetole 812 resin (Nissin-EM, Tokyo, Japan) at R.T. Finally, embedded slices were cured at 60°C for 3–4 days. Ultrathin sections (80 nm thick) were stained with uranyl acetate and lead citrate and exmamined in JEM 1010 electron microscope (JEOL, Tokyo, Japan).

Statistical Analysis

Statistical comparison between two independent groups of data was performed with the Student's *t*-test. Statistically significant differences are denoted $*P < 0.05$, $**P < 0.01$, and $***P < 0.001$ in all the figures.

RESULTS

Time Course of Expression Changes in Synapse- and Cytoskeleton-Related Genes After Repetitive Glutamate Stimulation

Gene expression changes induced by repetitive stimulation were first monitored by comparing expression profiles of three times glutamate-stimulated slices ([3G] slices) with those of three times mock-stimulated slices ([3C] slices) using the custom oligonucleotide DNA microarray synaptoarray containing probes for ~300 genes mainly involved in the construction and functioning of synapses (Takahashi et al., 2005; Kitamura et al., 2007; a complete list of genes on the microarray is supplied as Supp. Info. Table I).

At each time point, RNA extracted from 30 each of [3C] and [3G] slices were compared by competitive hybridization. To reduce individual variations, slices obtained from each animal were equally divided between [3C] and [3G] preparations. Because our preliminary experiment showed that significant changes in gene expression profiles were not detected at 1 hr after the third stimulation (3G1h), seven time points between 4 hr and 12 days after the third stimulation (4 hr, 24 hr, 48 hr, 96 hr, 6 days, 9 days, 12 days) were selected for analysis together with 26 hr after the second stimulation as a standard time point before the third stimulation (Fig. 1).

From the results of competitive hybridization, genes showing more than 50% up- or down-regulation at least once during the experimental time course were selected for further analysis (total of 77 genes). By k-means clustering, these 77 genes were classified into four groups (I–IV) with typical expression profiles as shown in Figure 2A,B. Comparison of these expression profiles revealed that changes in gene expression after the third stimulation occurred in two phases, an early

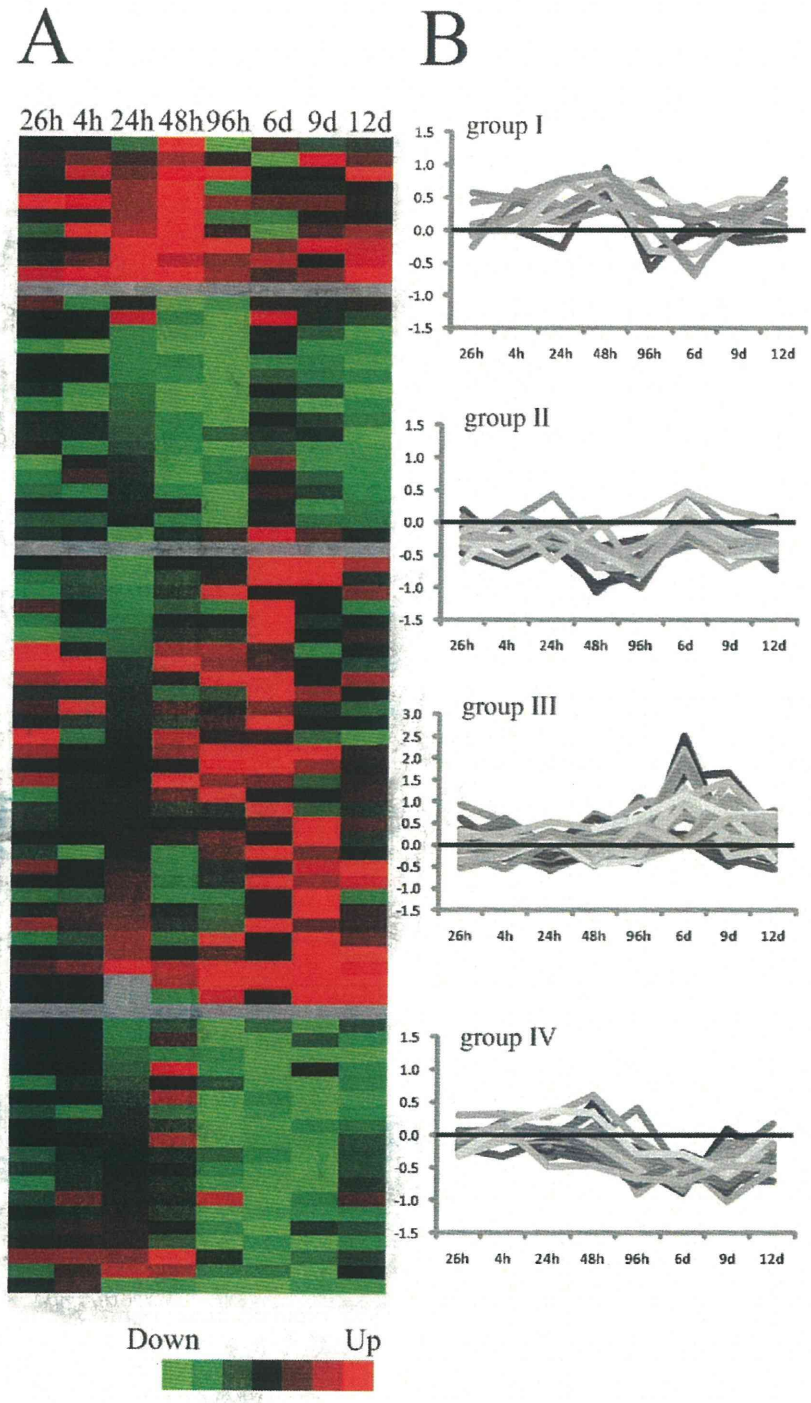

Fig. 2. Expression profiles of synapse- and cytoskeleton-related genes after repetitive stimulation. **A:** Classification of genes into four groups according to expression patterns by k-means clustering (k = 4). Genes showing more than 50% up-regulation (red) or down-regulation (green) in the three times glutamate-stimulated slices (3G) relative to mock-stimulated slices (3C) are colored. **B:** Time course of expression changes of individual genes in each group. For each gene, average expression ratios at each time point are expressed in logarithm of base 2 ($\log_2$ [3G]/[3C]) and plotted. Sampling time points between 4 hr and 12 days after the third stimulation are shown on the abscissa, with 26 hr representing the standard time point at 26 hr after the second stimulation.

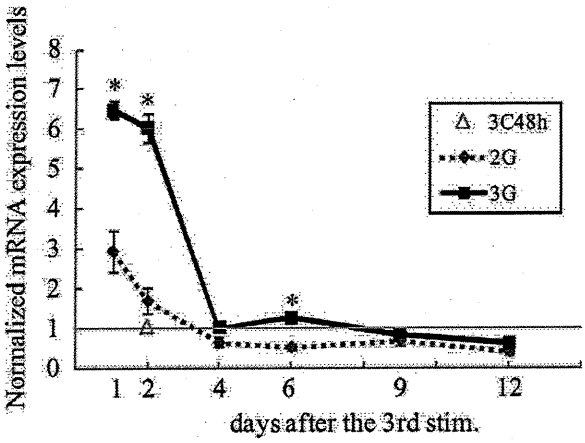

Fig. 3. Differences in the expression profiles of *bdnf* mRNA following two and three glutamate stimulations. Expression levels of *bdnf* mRNA in [2G] slices (lozenges) and [3G] slices (squares) at different time points after the last stimulation (day 0) were analyzed by real-time PCR using *rpL13a* as an internal standard and plotted relative to the level of *bdnf* mRNA in the control [3C] slices at 48 hr (triangle; mean ± SEM; n = 6, from two independent series of cultures).

phase (24 hr, 48 hr and 96 hr) and a late phase (6, 9, and 12 days). In the early phase, a peak of up-regulation was observed at 48 hr (group I), and the strongest down-regulation was observed at 48–96 hr (group II). In the late phase, significant up-regulation of group III genes was observed at 6–9 days. Group IV genes were persistently down-regulated between 96 hr and 9 days.

In the previous study, Tominaga-Yoshino et al. (2008) followed the course of synaptic enhancement after repetitive glutamate stimulation electrophysiologically and found that, after a decline of the initial enhancement of fEPSP (LTP) within 4 hr, there was a second and persistent enhancement of fEPSP (RISE) starting from 24 hr after the third stimulation and lasting for more than 3 weeks. An increase in the number of synaptic sites was also detected at 5 days after the third stimulation. Gene expression changes in the early phase may thus contribute primarily to the conversion from the transient LTP to the RISE.

Differences in the Expression Profiles of *bdnf* mRNA in Twice- and Thrice-Stimulated Slices

As one of the key factors regulating activity-dependent changes at the synapse, we compared expression profiles of *bdnf* mRNA in [2G] and [3G] slices by real-time PCR (Fig. 3). At 24 hr after the last stimulation, strong up-regulation of *bdnf* mRNA was observed in both [2G] and [3G] slices. Up-regulation in [3G] slices was much greater and persisted longer than that in [2G]slices. At 96 hr, *bdnf* expression in both types of slices was back to the baseline level. In [3G] slices, however, there was a small but significant second up-regulation at day 6. The earlier of the two phases of gene expression changes observed in Figure 2 thus corresponds to the first large peak of *bdnf* expression.

Comprehensive Screening of Gene Expression Changes 48 Hours After the Third Stimulation

From the time course analysis described above (Figs. 2, 3), we chose 48 hr after the third stimulation as a fixed time point at which to investigate thoroughly the genes responsible for the establishment of RISE using commercially available high-density arrays (Agilent Technologies). To make sure that the observed expression changes were not reflecting the apoptotic process induced by stimulation with high concentrations of glutamate in vitro (Schubert and Piasecki, 2001), histological evaluation of cell viability and analysis of caspase 3 (*casp3*) gene expression (Kroemer and Martin, 2005) were performed at this time point. As shown in Figure 4A, there was no significant difference in cell viability observed between slices experiencing three glutamate stimulations (3G48h) or three mock stimulations (3C48h), while slices exposed to 100 μM kainic acid for 24 hr exhibited significant incorporation of propidium iodide (PI), indicating cell death (Sakaguchi et al., 1997). Real-time PCR analysis further showed that the expression level of *casp3* in [3G] slices did not differ significantly from that of [3C] or [2G] slices (Fig. 4B). These data thus confirm that the glutamate stimulation protocol used in this study did not induce *casp3*-dependent apoptosis.

To increase efficiency and reliability of comprehensive screening, differentially stimulated slices were compared in two pairs by competitive hybridization 48 hr after the last stimulation, [3G] slices vs. [3C] slices and [3G] slices vs. [2G] slices. By focusing on differentially expressed genes detected in both pairs, genes progressively up- or down-regulated by repetitive stimulation and genes affected specifically by the third stimulation should be identified. Among the 22,575 gene probes on the high-density array, probes with signal intensities above 500 in both samples of the pair were selected for further analysis, and only probes showing consistent expression ratios of more than 1.2 (up-regulated) or less than 0.83 (down-regulated) were selected as differentially expressed. As a result, 1,437 up-regulated and 1,906 down-regulated probes were detected in the 3G vs. 3C comparison, whereas 1,136 up-regulated and 1,193 down-regulated probes were detected in the 3G /vs. 2G comparison (Supp. Info. Fig. 2A). Among these two pairs of comparisons, 701 up-regulated probes (3.1% of total probes) and 557 down-regulated probes (2.5%) were shared (Supp. Info. Fig. 2B), which were considered as candidate genes responding to repetitive stimulation.

We focused, among the candidate genes, on those up-regulated by more than two-fold in either pair of comparisons (3G/3C or 3G/2G), which amounted to 289. By deleting genes of unknown function, we finally ended up with a list of 176 putative repetitive stimula-

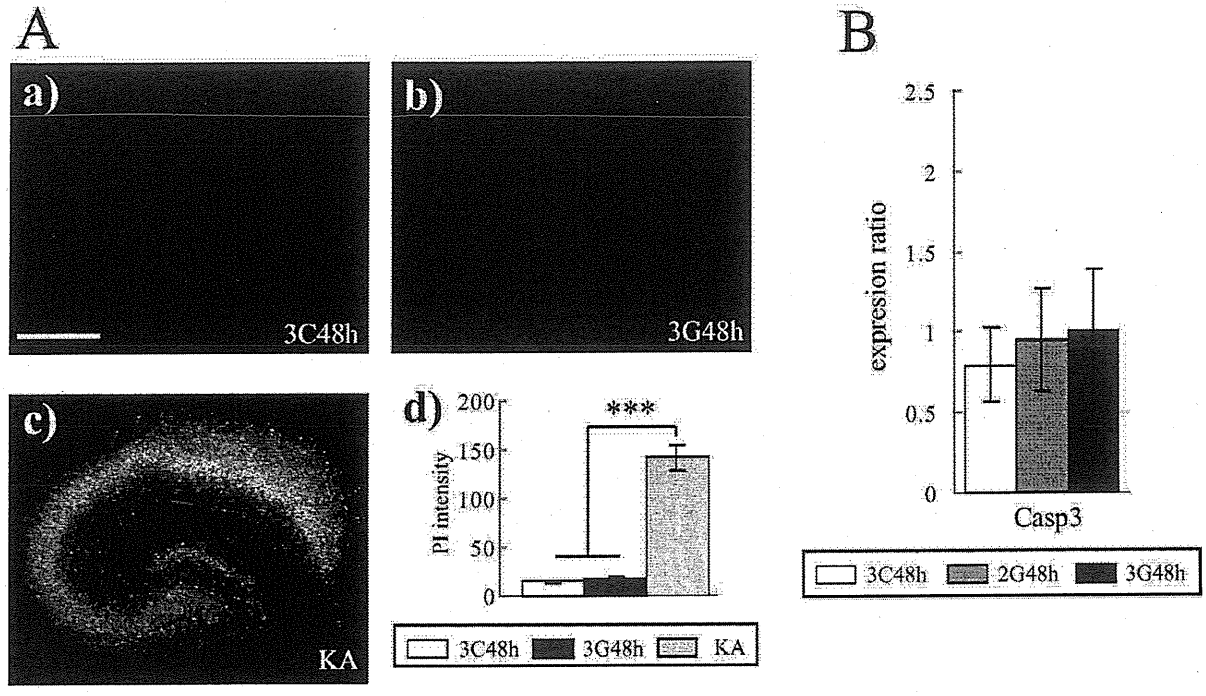

Fig. 4. Confirmation of cell viability after repetitive stimulation. **A:** Histochemical confirmation of cell viability by the absence of propidium iodide (PI) staining. Three times mock-stimulated ([3C]; a) or glutamate-stimulated ([3G]; b) hippocampal slices at 24 hr after the third stimulation were further incubated in culture medium containing 10 μg/ml PI for 24 hr at 34°C. A slice exposed to 100 μM kainic acid for 24 hr in the presence of PI is shown as a positive control (KA; c). In d, total PI fluorescence of each micrograph was quantified in NIH Image software (mean ± SEM; n = 3). **B:** Real-time quantitative PCR analysis of *casp3* in [3C], [2G], and [3G] slices at 48 hr after the last stimulation using *rpL13a* as an internal standard (mean ± SEM; n = 6, from two independent series of cultures). Scale bar = 500 μm.

tion-induced genes (provided as Supp. Info. Table III). Several genes previously reported to be induced by physiological/unphysiological stimuli or behavioral conditionings and to be correlated with synaptic plasticity and memory were found on this list; *grm5* (type 1 metabotropic glutamate receptor 5; Manahan-Vaughan et al., 2003), *rgs2* (regulator of G-protein signaling; Ingi et al., 1998), *syt4* (synaptotagmin-4; Vician et al., 1995), and *ania4/carp/dclk1* (doublecortin-like kinase 1; Berke et al., 1998; Vreugdenhil et al., 1999). Though not as highly up-regulated as those on the list, three other genes known to be activity-induced were also included in the 701 candidate up-regulated genes, *bdnf* (brain-derived neurotrophic factor; Hall et al., 2000), *cpg1* (candidate plasticity-related gene 1; Nedivi et al., 1993), and *rheb* (rapidly and transiently induced gene in hippocampal granule cells; Yamagata et al., 1994). In addition to these activity-related genes, *ywhaz/14-3-3ζ* (tyrosine 3-monooxygenase/tryptophan 5-monooxygenase activation protein, zeta polypeptide) involved in the regulation of actin dynamics (Soosairajah et al., 2005) and *slc6a11* (neurotransmitter transporter, GABA, member 11) were among the 176 highly up-regulated genes.

To confirm microarray data, real-time quantitative PCR analysis was performed with the six representative highly up-regulated genes mentioned above (*grm5, rgs2, syt4, ania4, ywhaz, slc6a11*) as well as the following two related genes, which were among the 701 up-regulated candidate genes; *slc6a12* (neurotransmitter transporter, betaine/GABA, member 12), and *gabarapl2* ($GABA_A$ receptor-associated protein-like 2). Expression ratios of [3G] and [2G] slices relative to [3C] slices at 48 hr after the last stimulation were obtained using *rpL13a* (60S ribosomal subunit protein gene) as internal stnadard, yielding results mostly consistent with microarray data (Fig. 5). Compared with the twice-stimulated sample, significant up-regulation by the third stimulation was observed with *syt4, ywhaz, slc6a12*, and *gabarapl2*. It is also noteworthy that *ania4, grm5*, and *syt4*, which have been reported to be induced by extensive stimulation (e.g., seizure), were up-regulated by repeating the weaker stimulation three times without induction of apoptosis (Fig. 4).

Increases in the Protein Levels of BDNF, GRM5, and SYT4 by Repetitive Glutamate Stimulation

We confirmed the expression of three repetitive stimulation-induced genes, *bdnf, grm5*, and *syt4*, at the protein level. As shown in Figure 6A, BDNF and mGluR5 proteins were increased both in [2G48h] slices

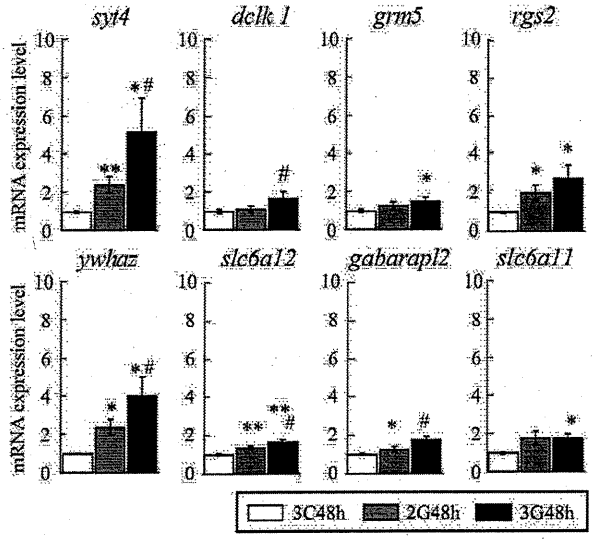

Fig. 5. Real-time quantitative PCR analysis of the representative genes. Repetitive stimulation-dependent changes in the expression of eight representative genes detected by microarray analyses were validated by real-time quantitative PCR. For each gene, average expression ratios of [2G] and [3G] slices relative to [3C] slices at 48 hr after the last stimulation (3G48h/3C48h or 2G48h/3C48h) are shown. All expression ratios were normalized with that of *rpL13a* as internal standard (mean ratio ± SEM; n = 6, from two independent series of cultures). Values with statistically significant differences compared with that of [3C] slices are marked $^{*}P < 0.05$ or $^{**}P < 0.01$, and those of [3G] slices compared with that of the [2G] slices are marked $^{\#}P < 0.05$.

and in [3G48h] slices, whereas Syt4 protein was increased only in [3G48h] slices. The third stimulation-specific increase of Syt4 was further confirmed by immunostaining the hippocampal slices with anti-Syt4 antibody as shown in Figure 6B. Consistent with the results of Western blotting, Syt4 immunoreactivity was significantly increased in [3G] slices compared with [3C] and [2G] slices. It is notable that the up-regulation of Syt4 was most prominent in the CA3 region, where it was localized to perikarya of pyaramidal neurons. Immunostaining at different time intervals after the third stimulation revealed that Syt4 was also up-regulated at 24 hr and 96 hr, but not at later time points of 6 days, 8 days, and 12 days (data not shown).

Coordinated Changes in the Expression of Genes Regulating Cofilin Phosphorylation Leading to Changes in Actin Polymerization

Because *ywhaz/14-3-3ζ* is known as a regulator of *ssh1l* (slingshot homolog 1) phosphatase that activates the actin depolymerizing factor cofilin, and cofilin was among the genes in group IV (Fig. 2), we investigated by real-time quantitative PCR the effect of repetitive stimulation on the expression of four additional genes involved in this pathway (Fig. 7A), *ssh1l, pak4* (p21 (CDKN1A)-activated kinase 4), *limk1* (LIM-domain containing protein kinase 1), and *cfl1* (cofilin 1, non-muscle). Although probes for these four genes were on the high-density array, sufficient signal intensities were not obtained.

Cofilin serves as one of the major stimulators of actin turnover and actin filament dynamics by enhancing depolymerization at the minus end and by severing actin filaments to produce new plus ends. Cofilin is inactivated through phosphorylation of the N-terminal Ser3 by LIMK1 and reactivated through dephosphorylation by SSH1. Activities of both of these enzymes are regulated through phosphorylation by PAK4, which activates LIMK1 and inactivates SSH1. Ywhaz, on the other hand, inhibits SSH1 activity by sequestering it in the cytoplasm. As summarized in Figure 7B, transcription of genes for all of these five proteins were up-regulated compared with control (3C) 48 hr after the second stimulation (2G), indicating that glutamate stimulation activated actin filament dynamics by up-regulating factors involved in both polymerization and depolymerization. In contrast, these genes were differentially affected by the third stimulation; *cfl1* and *ssh1l* were down-regulated, whereas *pak4, ywhaz*, and *limk1* were further up-regulated. This should lead to suppression of actin filament dynamics and enhancement of actin polymerization through cofilin phosphorylation as summarized in Figure 7B.

To confirm the involvement of cofilin phosphorylation in the third-stimulation-specific RISE phenomenon, we examined the phosphorylation states of cofilin by Western blotting using the phosphorylated cofilin-specific antibody (Fig. 7C). Consistent with the expression profiles of actin dynamics regulators, the phosphorylation level of cofilin was significantly reduced after the second stimulation (2G48h) compared with the control (3C48h). Conversely, the phosphorylation level of cofilin showed a tendency to increase after the third stimulation (3G48h) compared with 2G48h. Estimation of the level of actin polymerization with fluorescently labeled phalloidin revealed that, consistent with changes in cofilin phosphorylation states, phalloidin staining was significantly decreased after the second stimulation (2G48h) compared with the control (3C48h) especially in the CA1 region (Fig. 7D). Conversely, intensity of phalloidin staining after the third stimulation (3G48h) was increased compared with 2G48h. In addition, direct observation of actin-containing filament structures in these slices by transmission electron microscopy after actin filament stabilization with phalloidin and tannic acid revealed an increase in the density of the 7–8-nm microfilament structures spreading from PSD and constructing the subsynaptic web in 3G48h slices compared with 2G48h slices (Fig. 7E). The results thus indicate that the second stimulation transiently destabilized the actin cytoskeleton, whereas the third stimulation suppressed actin filament dynamics and enhanced actin polymerization.

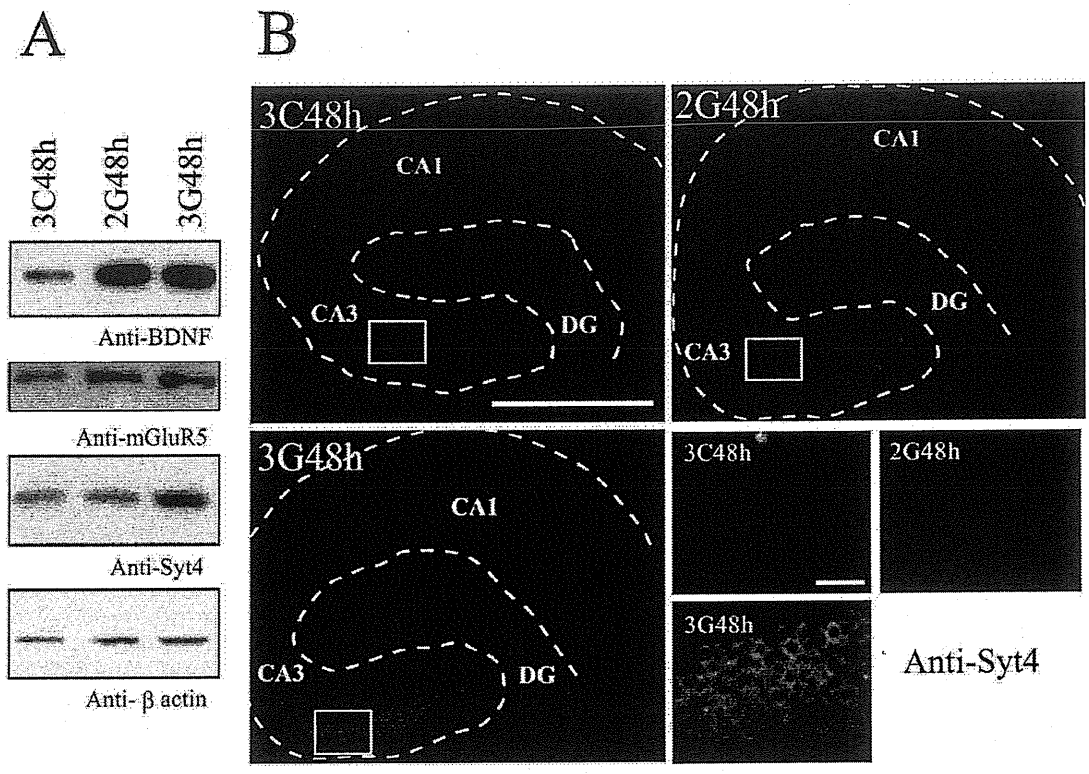

Fig. 6. **A,B:** Increases in the protein levels of BDNF, mGluR5, and Syt4 by repetitive glutamate stimulation. The lysate of the [3C], [2G], or [3G] slices obtained 48 hr after the last stimulation was analyzed by Western blotting with the antibodies against BDNF, mGluR5, Syt4, or β-actin as indicated. The [3C], [2G], and [3G] hippocampal slices 48 hr after the last stimulation were immunostained with anti-Syt4 antibody. The dashed line indicates the edge of the slice. Boxed regions are shown at higher magnification at the lower right corner. Scale bars = 500 μm in larger panels; 50 μm in smaller panels.

DISCUSSION

Correlations Among Genes Induced by Repetitive Stimulation, LTP, and Epileptic Activity

Because RISE develops after the repeated induction of LTP, several genes previously reported to be up-regulated during LTP induction in vitro or in vivo were detected among genes up-regulated by repetitive stimulation, as expected: *bdnf*, which has been shown to increase by the stimulus paradigm inducing LTP in CA1 in vitro and by contextual learning in vivo (Hall et al., 2000); *rgs2* (regulator of G protein signaling 2); and *grm5* (type1 metabotropic glutamate receptor 5) were induced following LTP induction in DG and CA1 in vivo (Manahan-Vaughan et al., 2003). In particular, larger and longer-lasting up-regulation by three repetitive stimulations compared with two was observed with *bdnf*, which has been shown to be a key factor in activity-dependent synaptic enhancement.

Furthermore, two genes reported to be induced in the hippocampus by kainate-elicited seizures were also up-regulated by repetitive stimulation; *ania 4/dclk 1* (Vreugdenhil et al., 1999) and *syt4* (Vician et al., 1995). *ania 4/dclk 1* Encodes a protein kinase similar to Ca^{2+}/calmodulin-dependent kinases (CAMK) but with an additional N-terminal doublecortin (DCX) homology domain. As with DCX, DCLK1 shows microtubule-binding and polymerization activities (Lin et al., 2000), suggesting that it may regulate neurite extension and cell migration. Syt4, on the other hand, has been shown recently to be localized to BDNF-containing vesicles and to regulate BDNF release negatively in response to synaptic activity (Dean et al., 2009). Such regulation by Syt4 may be a mechanism to avoid exhaustive stimulation and maintain the level of BDNF as well as synaptic strength in a useful range during long-lasting LTP. In contrast to kainate-induced seizures, which resulted in strong up-regulation of Syt4 protein in CA1, CA3, and DG in vivo (Vician et al., 1995), repetitive glutamate stimulation induced prominent up-regulation only in the CA3 region (Fig. 6B). The repetitive glutamate stimulation protocol used in this study thus achieved induction of genes that are dependent on stronger or nonphysiological stimuli without induction of excitotoxic cell death (Fig. 4). Insofar as epileptic seizures have also been reported to up-regulate *bdnf* (Kokaia et al., 1994; Poulsen et al., 2004), results of the present study indicate that the long-lasting synaptic enhancement induced by repet-

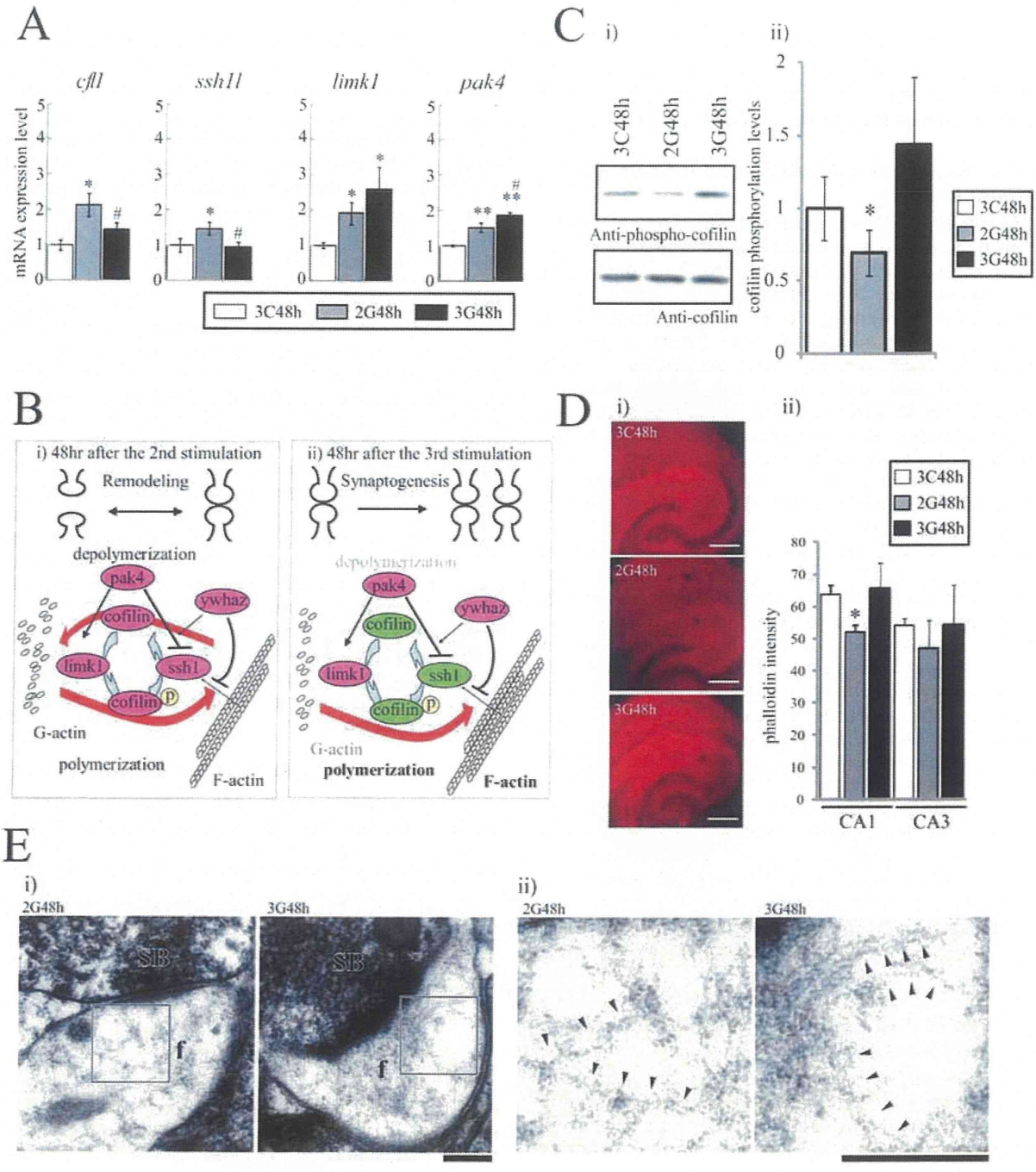

Fig. 7. Expression changes of genes involved in the regulation of actin dynamics by repetitive stimulation. **A:** Real-time PCR analysis of the differences in the expression of an additional four genes involved in the regulation of actin dynamics. For each gene, average expression ratios of [2G] and [3G] slices relative to [3C] slices at 48 hr after the last stimulation are shown (mean ± SEM; n = 6, from two independent series of cultures). All expression ratios were normalized with that of *rpL13a*. Values with statistically significant differences compared with the [3C] slices are marked $^{*}P < 0.05$ or $^{**}P < 0.01$, and those of [3G] slices compared with that of [2G] slices are marked $^{\#}P < 0.05$). **B:** Schematic representation of the regulation of actin filament dynamics after repetitive stimulation showing stimulatory (arrows) and inhibitory (blocked lines) interactions among the five genes. i) After two stimulations, five genes regulating actin dynamics were all up-regulated, indicating that both polymerization and depolymerization of actin were enhanced. ii) Three stimulations coordinately changed the expression of five genes to suppress actin depolymerization and enhance polymerization (cfl1 and SSH1 were down-regulated; PAK4, Ywhaz, and LIMK1 were up-regulated). **C:** i) Phosphorylation level of cofilin protein was analyzed by Western blotting with the antibodies against phosphophorylated cofilin (at Ser 3) and total cofilin as indicated. ii) Phosphorylation levels of cofilin were quantified by the ratio of phosphorylated-cofilin to total cofilin (mean ± SEM; n = 4). Values with statistically significant differences compared with [3C] slices are marked $^{*}P < 0.05$. **D:** i) The [3C], [2G], and [3G] hippocampal slices 48 hr after the last stimulation were stained with Alexa 594-conjugated phalloidin selective for F-actin. ii) Relative intensities of fluorescent phalloidin staining in CA1 and CA3 regions of [3C], [2G], and [3G] slices 48 hr after the last stimulation. Values with statistically significant differences compared with [3C] slices are marked $^{*}P < 0.05$. **E:** Electron microscopic analysis confirms the increase in the actin filament structures after repeated glutamate exposures. i) The 7–8-nm microfilaments spread from PSD and constructed subsynaptic web (f). Boxed areas in i are enlarged in ii. SB indicates presynaptic bouton. Arrowheads in ii indicate thin microfilaments extending from the web. Scale bars = 300 μm in D; 200 nm in E.

itive glutamate stimulation at least partially shares the common pathways leading to LTP and epileptic activity.

Effect of Repetitive Stimulation on GABAergic Neurotransmission

In addition to the positive modulations of excitatory synapses, negative modulations of inhibitory synapses have been shown to contribute to the induction of LTP (Casasola et al., 2004; Fiumelli et al., 2005). In our comprehensive screening, three genes involved in GABAergic neurotransmission were found to be up-regulated by repetitive glutamate stimulation; GABA transporters *slc6a12* and *slc6a11* and GABA receptor-interacting protein *gabarapl2* (Fig. 5). Up-regulation of GABA transporters may attenuate the inhibitory action of GABA by reducing its synaptic concentration.

The inhibitory nature of GABAergic transmission depends on the transmembrane Cl^- gradient, which is regulated mainly by the neuron-specific K^+-Cl^- cotransporter KCC2 responsible for Cl^- extrusion. A positive shift in the Cl^- reversal potential through activity-dependent suppression of KCC2 function (Fiumelli et al., 2005) as well as its gene expression (Rivera et al., 2004) is thus considered as one of the major mechanisms of activity-induced negative modification in inhibitory synapses. In our microarray analysis, *Slc12a5/KCC2* was found to be down-regulated to a similar degree after the second and the third stimulations (data not shown).

Kleschevnikov et al. (2004) have shown that the high-frequency stimulation (HFS) inducing LTP under normal conditions produced epileptiform activity in the presence of $GABA_A$ receptor antagonist picrotoxin (Kleschevnikov et al., 2004). A shift in the balance between excitatory and inhibitory pathways through attenuation of GABAergic neurotransmission may thus be another common basis for the induction of LTP, epileptic activity, and long-lasting synaptic enhancement by repetitive stimulation.

Modulation of Actin Filament Dynamics Leading to Structural Reorganization

Previous studies have shown that stimulation paradigms inducing LTP are associated with reorganization of the actin cytoskeleton characterized by an increase in filamentous actin (F-actin) content within dendritic spines (Fukazawa et al., 2003). In most cases, these changes were temporary and accomplished by the modification or translocation of the proteins associated with the actin cytoskeleton. In our time course analysis, however, numerous genes involved in the regulation of the actin cytoskeleton were found to change expression levels during the early phase after stimulation. In particular, five genes modulating the dynamics of actin polymerization through the cofilin pathway were found to be coordinately but differentially regulated at 48 hr after the second and the third stimulations (Figs. 5, 7); all five genes were up-regulated after the second stimulation, whereas *cfl1* and *ssh1l* were down-regulated and *ywhaz/14-3-3ζ*, *pak4*, and *limk1* were up-regulated after the third stimulation. Cofilin 1 is an actin-depolymerizing factor, which increases actin dynamics by severing actin filaments and binding to the severed plus ends. Cofilin1 is inactivated by LIM-kinase 1 through phosphorylation at Ser-3 and is reactivated by the phosphatase slingshot 1L, which, in turn, is inhibited by the kinase PAK4 and the ywhaz protein (Nagata-Ohashi et al., 2004). On the other hand, PAK4 kinase activates LIMK1 to regulate cooperatively the phosphorylation state of cofilin1 (Soosairajah et al., 2005). The observed expression changes in these genes after the second stimulation enhance actin dynamics by enhancing both polymerization and depolymerization, whereas changes after the third stimulation coordinately decrease the activity of cfl1 to slow actin dynamics and stabilize F-actin. Consistent with the gene expression profiles of actin dynamics regulators, cofilin phosphorylation and intensity of phalloidin staining (F-actin) were significantly reduced after the second stimulation compared with the control (3C48h). Conversely, cofilin phosphorylation, intensity of phalloidin staining, and actin microfilament structures were increased after the third stimulation compared with 2G48h (Fig. 7). These results thus indicate that stabilization of actin dynamics through cofilin phosphorylation underlies the structural reorganization leading to the establishment of RISE, the repetitive stimulation-induced long-lasting synaptic enhancement.

ACKNOWLEDGMENTS

The authors thank Mr. Tomoyuki Amemiya (RIKEN) for his assistance in the development of the DNA microarray; Dr. Masaki Takahashi (Aoyama Gakuin University) for valuable suggestions and help in microarray analysis during the initial phase of the study; and Dr. Takayuki Negishi, Ms. Madoka Inoue, and Mr. Hajime Shirane (Aoyama Gakuin University) for their assistance in designing primers for real-time quantitative PCR.

REFERENCES

Bear MF, Connors BW, Paradiso MA. 2001. Neuroscience: exploring the brain, 2nd ed. Baltimore: Lippincott Williams & Wilkins.

Berke JD, Paletzki RF, Aronson GJ, Hyman SE, Gerfen CR. 1998. A complex program of striatal gene expression induced by dopaminergic stimulation. J Neurosci 18:5301–5310.

Casasola C, Montiel T, Calixto E, Brailowsky S. 2004. Hyperexcitability induced by GABA withdrawal facilitates hippocampal long-term potentiation. Neuroscience 126:163–171.

Collingridge GL, Isaac JT, Wang YT. 2004. Receptor trafficking and synaptic plasticity. Nat Rev Neurosci 5:952–962.

Dean C, Liu H, Mark Dunning F, Chang PY, Jackson MB, Chapman ER. 2009. Synaptotagmin-IV modulates synaptic function and long-term potentiation by regulating BDNF release. Nat Neurosci (in press).

DeRisi J, Penland L, Brown PO, Bittner ML, Meltzer PS, Ray M, Chen Y, Su YA, Trent JM. 1996. Use of a cDNA microarray to analyse gene expression patterns in human cancer. Nat Genet 14:457–460.

Dino MR, Mugnaini E. 2000. Postsynaptic actin filaments at the giant mossy fiber-unipolar brush cell synapse. Synapse 38:499–510.

Fiumelli H, Cancedda L, Poo MM. 2005. Modulation of GABAergic transmission by activity via postsynaptic Ca^{2+}-dependent regulation of KCC2 function. Neuron 48:773–786.

Frey U, Frey S, Schollmeier F, Krug M. 1996. Influence of actinomycin D, a RNA synthesis inhibitor, on long-term potentiation in rat hippocampal neurons in vivo and in vitro. J Physiol 490:703–711.

Fukazawa Y, Saitoh Y, Ozawa F, Ohta Y, Mizuno K, Inokuchi K. 2003. Hippocampal LTP is accompanied by enhanced F-actin content within the dendritic spine that is essential for late LTP maintenance in vivo. Neuron 38:447–460.

Gahwiler BH, Capogna M, Debanne D, McKinney RA, Thompson SM. 1997. Organotypic slice cultures: a technique has come of age. Trends Neurosci 20:471–477.

Hall J, Thomas KL, Everitt BJ. 2000. Rapid and selective induction of BDNF expression in the hippocampus during contextual learning. Nat Neurosci 3:533–535.

Ingi T, Krumins AM, Chidiac P, Brothers GM, Chung S, Snow BE, Barnes CA, Lanahan AA, Siderovski DP, Ross EM, Gilman AG, Worley PF. 1998. Dynamic regulation of RGS2 suggests a novel mechanism in G-protein signaling and neuronal plasticity. J Neurosci 18:7178–7188.

Kawaai K, Hisatsune C, Kuroda Y, Mizutani A, Tashiro T, Mikoshiba K. 2009. 80K-H interacts with inositol 1,4,5-trisphosphate (IP3) receptors and regulates IP3-induced calcium release activity. J Biol Chem 284:372–380.

Kitamura C, Takahashi M, Kondoh Y, Tashiro H, Tashiro T. 2007. Identification of synaptic activity-dependent genes by exposure of cultured cortical neurons to tetrodotoxin followed by its withdrawal. J Neurosci Res 85:2385–2399.

Klann E, Dever TE. 2004. Biochemical mechanisms for translational regulation in synaptic plasticity. Nat Rev Neurosci 5:931–942.

Kleschevnikov AM, Belichenko PV, Villar AJ, Epstein CJ, Malenka RC, Mobley WC. 2004. Hippocampal long-term potentiation suppressed by increased inhibition in the Ts65Dn mouse, a genetic model of Down syndrome. J Neurosci 24:8153–8160.

Kokaia Z, Metsis M, Kokaia M, Bengzon J, Elmer E, Smith ML, Timmusk T, Siesjo BK, Persson H, Lindvall O. 1994. Brain insults in rats induce increased expression of the BDNF gene through differential use of multiple promoters. Eur J Neurosci 6:587–596.

Kroemer G, Martin SJ. 2005. Caspase-independent cell death. Nat Med 11:725–730.

Lin PT, Gleeson JG, Corbo JC, Flanagan L, Walsh CA. 2000. DCAMKL1 encodes a protein kinase with homology to doublecortin that regulates microtubule polymerization. J Neurosci 20:9152–9161.

Lisman J, Schulman H, Cline H. 2002. The molecular basis of CaMKII function in synaptic and behavioural memory. Nat Rev Neurosci 3:175–190.

Lynch MA. 2004. Long-term potentiation and memory. Physiol Rev 84:87–136.

Manahan-Vaughan D, Ngomba RT, Storto M, Kulla A, Catania MV, Chiechio S, Rampello L, Passarelli F, Capece A, Reymann KG, Nicoletti F. 2003. An increased expression of the mGlu5 receptor protein following LTP induction at the perforant path-dentate gyrus synapse in freely moving rats. Neuropharmacology 44:17–25.

Maupin-Szamier P, Pollard TD. 1978. Actin filament destruction by osmium tetroxide. J Cell Biol 77:837–852.

Mbassa G, Elger M, Kriz W. 1988. The ultrastructural organization of the basement membrane of Bowman's capsule in the rat renal corpuscle. Cell Tissue Res 253:151–163.

Muller D, Buchs PA, Stoppini L. 1993. Time course of synaptic development in hippocampal organotypic cultures. Brain Res Dev Brain Res 71:93–100.

Nagata-Ohashi K, Ohta Y, Goto K, Chiba S, Mori R, Nishita M, Ohashi K, Kousaka K, Iwamatsu A, Niwa R, Uemura T, Mizuno K. 2004. A pathway of neuregulin-induced activation of cofilin-phosphatase Slingshot and cofilin in lamellipodia. J Cell Biol 165:465–471.

Nedivi E, Hevroni D, Naot D, Israeli D, Citri Y. 1993. Numerous candidate plasticity-related genes revealed by differential cDNA cloning. Nature 363:718–722.

Otani S, Marshall CJ, Tate WP, Goddard GV, Abraham WC. 1989. Maintenance of long-term potentiation in rat dentate gyrus requires protein synthesis but not messenger RNA synthesis immediately post-tetanization. Neuroscience 28:519–526.

Poulsen FR, Lauterborn J, Zimmer J, Gall CM. 2004. Differential expression of brain-derived neurotrophic factor transcripts after pilocarpine-induced seizure-like activity is related to mode of Ca^{2+} entry. Neuroscience 126:665–676.

Rivera C, Voipio J, Thomas-Crusells J, Li H, Emri Z, Sipila S, Payne JA, Minichiello L, Saarma M, Kaila K. 2004. Mechanism of activity-dependent downregulation of the neuron-specific K-Cl cotransporter KCC2. J Neurosci 24:4683–4691.

Sakaguchi T, Okada M, Kuno M, Kawasaki K. 1997. Dual mode of N-methyl-D-aspartate-induced neuronal death in hippocampal slice cultures in relation to N-methyl-D-aspartate receptor properties. Neuroscience 76:411–423.

Schubert D, Piasecki D. 2001. Oxidative glutamate toxicity can be a component of the excitotoxicity cascade. J Neurosci 21:7455–7462.

Shinoda Y, Tominaga-Yoshino K, Ogura A. 2003. The dendritic layer-specific persistent enhancement of synaptic transmission induced by repetitive activation of protein kinase A. Neurosci Res 47:191–200.

Soosairajah J, Maiti S, Wiggan O, Sarmiere P, Moussi N, Sarcevic B, Sampath R, Bamburg JR, Bernard O. 2005. Interplay between components of a novel LIM kinase-slingshot phosphatase complex regulates cofilin. EMBO J 24:473–486.

Steward O, Schuman EM. 2001. Protein synthesis at synaptic sites on dendrites. Annu Rev Neurosci 24:299–325.

Takahashi M, Kondoh Y, Tashiro H, Koibuchi N, Kuroda Y, Tashiro T. 2005. Monitoring synaptogenesis in the developing mouse cerebellum with an original oligonucleotide microarray. J Neurosci Res 80:777–788.

Tominaga-Yoshino K, Kondo S, Tamotsu S, Ogura A. 2002. Repetitive activation of protein kinase A induces slow and persistent potentiation associated with synaptogenesis in cultured hippocampus. Neurosci Res 44:357–367.

Tominaga-Yoshino K, Urakubo T, Okada M, Matsuda H, Ogura A. 2008. Repetitive induction of late-phase LTP produces long-lasting synaptic enhancement accompanied by synaptogenesis in cultured hippocampal slices. Hippocampus 18:281–293.

Urakubo T, Ogura A, Tominaga-Yoshino K. 2006. Ultrastructural features of hippocampal CA1 synapses with respect to synaptic enhancement following repeated PKA activation. Neurosci Lett 407:1–5.

Vician L, Lim IK, Ferguson G, Tocco G, Baudry M, Herschman HR. 1995. Synaptotagmin IV is an immediate early gene induced by depolarization in PC12 cells and in brain. Proc Natl Acad Sci U S A 92:2164–2168.

Vreugdenhil E, Datson N, Engels B, de Jong J, van Koningsbruggen S, Schaaf M, de Kloet ER. 1999. Kainate-elicited seizures induce mRNA encoding a CaMK-related peptide: a putative modulator of kinase activity in rat hippocampus. J Neurobiol 39:41–50.

Yamagata K, Sanders LK, Kaufmann WE, Yee W, Barnes CA, Nathans D, Worley PF. 1994. rheb, A growth factor- and synaptic activity-regulated gene, encodes a novel Ras-related protein. J Biol Chem 269:16333–16339.

In: Bananas: Nutrition, Diseases and Trade Issues
Editor: Alisha E. Cohen
ISBN 978-1-61761-124-7

Chapter 12

HYPERKALEMIA AND HYPERDOPAMINEMIA ALONG WITH PSYCHOLOGICAL MODIFICATION INDUCED BY OBSESSIVE EATING OF BANANAS IN AN ANOREXIA NERVOSA ADOLESCENT

Naoko Narita[1,] Mami Tazoe[2,†], and Masaaki Narita[3,‡]*
[1]Institute of Education, Bunkyo University, 3337 Minamiogishima, Koshigaya-City, Saitama, 343-8511, Japan
[2]Department of Clinical Psychology, Japan Lutheran College, 3-10-20 Osawa, Mitaka, Japan
[3]Developmental and Regenerative Medicine, Mie University, 2-174, Edobashi, Tsu, 514-8507, Japan

ABSTRACT

Bananas are known as a dopamine-rich and potassium-rich food, however no previous data regarding biochemical or psychological alteration induced by excess intake of bananas has been reported. We encountered a female adolescent patient with anorexia nervosa, who was obsessed by an extremely restricted eating habit. As a result of ingesting nothing but a maximum of 20 bananas and less than 500 ml of mineral water per day for more than two years, she exhibited biochemical and metabolic disorders such as hyperkalemia, hyperdopaminemia, and pseudoaldosteronism. The patient also showed a drastic change in her psychological state, represented by decreased anxiety and increase in inner-impulse. Based on the biochemical changes seen in the patient, the accumulation of free dopamine due to obsessive banana ingestion was the most likely cause of her

* Author for correspondence. MD, PhD, Telephone: +81-48-974-8811; Fax : +81-48-974-8960; E-mail : nnarita@koshigaya.bunkyo.ac.jp
† MS. Telephone: +81-422-31-4611; Fax: +81-422-33-6405; E-mail: mtazoe@luther.ac.jp

altered psychological state. When the patient resumed eating other food items after 26 months of obsessive and restricted banana ingestion, the abnormalities in her blood values and her psychological state were corrected to that of the pre-obsessive eating period. We conclude that in this case, an obsessive and restricted eating habit of banana ingestion modulated her biological and psychological homeostasis.

INTRODUCTION

Eating disorders, which are subcategorized in the Diagnostic and Statistical Manual of Mental Disorders, Fourth Edition (DSM-IV) as anorexia nervosa, bulimia nervosa, and eating disorder not otherwise specified, are characterized by unusual eating habits caused by an intense fear of becoming fat (American Psychiatric Association, 1994). Although the precise etiology of eating disorders is unclear, abnormalities of biogenic amine neurotransmitters such as serotonin (5-hydroxytryptamine, 5-HT) and dopamine are found in some patients (Brewerton and Jimerson, 1996; Kaye et al 1999; Wolfe et al 2000), suggesting the relevance of these factors to eating habits. Since an abnormal eating habit is the essential phenotype of eating disorders (Behrman et al 2000), the occurrence of obsessive eating habits in patients with eating disorders is not surprising (Kaye, 2008).

Anorexia nervosa is characterized by self-imposed weight loss and amenorrhea. A distorted psychopathologic attitude toward eating and body weight is pathognomonic of anorexia nervosa. (Behrman et al 2000). DSM-IV (American Psychiatric Association, 1994) classifies anorexia nervosa into a restricting type and binge-eating/purging type based on the presence of binge-eating/purging (rapid consumption of large amounts of food, followed by induced vomiting or misuse of laxatives). In DSM-IV, bulimia nervosa is distinguished from anorexia nervosa based on the clinical manifestations, although the psychological background including excessive concern about body shape and weight is common to both. In contrast to the emaciation generally observed in anorexia nervosa patients, bulimia nervosa patients hardly manifest noticeable under- or overweight. The DSM-IV criteria define bulimia nervosa as follows: the binge-eating/purging episodes are observed at intervals of less than 2 hours, and the patient has a minimum average of two episodes per week for at least 3 months.

Anorexia nervosa and bulimia nervosa patients share particular eating habits including binge eating, restricted food selection, and obsessive eating. Dysfunction of serotonergic or dopaminergic neuronal systems is the most likely pathophysiologic process in these disorders (Bosanac et al 2005). The serotonergic neuronal system originates from the midbrain raphe nucleus, and its projection regulates diverse physiologic functions, including sleep, appetite, pain, motor function, cognition, sexual activity, and emotions such as mood and anxiety. Decreased activity of the serotonergic neuronal system is often observed in patients with eating disorders (Fumeron et al 2001; Sorbi et al 1998). On the other hand, the dopaminergic neuronal system has a role in cognition, locomotor activity, exploration, motivation, feeding, and sexual behavior. Activation of the dopaminergic neuronal system in restricting anorexia nervosa patients has been suspected based on their clinical manifestations and the increase of dopamine metabolites observed in their cerebrospinal fluid (Devesa et al 1988; Kaye et al 1999). However, no conclusive evidence is available to date.

‡ MD, PhD. Telephone: +81-59-232-1111; Fax: +81-59-232-8031; E-mail: narita_m@doc.medic.mie-u.ac.jp

It is conceivable that the frequent co-morbidity of anorexia nervosa / bulimia nervosa with other psychiatric disorders is quite relevant to abnormalities of serotonergic / dopaminergic systems. For instance, it is fairly common to observe food- and weight-related obsessive-compulsive symptoms during the course of anorexia nervosa. Patients with anorexia nervosa often are obsessed with calculating calories, searching for low-calorie food, or performing obviously excessive amounts of exercise. All of these features can be interpreted as phenotypes of obsessive-compulsive disorder or obsessive-compulsive personality disorder. Recent neurobiological, genetic, and psychological investigations have accumulated evidence of an overlapping spectrum between anorexia nervosa, bulimia nervosa, and binge eating disorder (originally classified in the eating disorders-NOS in DSM-IV) and obsessive-compulsive disorder or obsessive-compulsive personality disorder (Lazaro et al 2005; Serpell et al 2002).

Prevalence rates for obsessive-compulsive disorder or obsessive-compulsive features in eating disorders are relatively high, ranging between 25–69% in anorexia nervosa, and 3–40% in bulimia nervosa (Lawson et al 2007). Abnormal eating habits such as restriction and binge eating themselves can be explained by compulsive behavior to achieve affect regulation (e.g., reducing anxiety). Therefore, there is a keen debate about the pertinence of separating eating disorders and obsessive-compulsive disorder as different diagnostic categories, because they are presently assigned to separate categories in DSM-IV (Grilo, 2004; Wu, 2008). Moreover, mood disorders, anxiety disorders, and personality disorders are more commonly present with bulimia nervosa than anorexia nervosa, suggesting that the etiologies of anorexia nervosa and bulimia nervosa are quite similar but not identical (Carlos et al 2009; Kaye, 2008). However, it is noteworthy that such disorders, which are possibly co-morbid with anorexia nervosa / bulimia nervosa, are also known to be caused, at least partially, by serotonergic neuronal dysregulation.

Obsessive eating in patients with bulimia nervosa / binge eating disorder is more likely to involve an obsession with the cycle of overeating and purging rather than with the food itself. This behavior can be understood to be similar to an addiction to drugs or other substances. Usually the patients experience regret and anguish after the binge eating episode, followed by inadequate compensatory behavior such as vomiting, laxative abuse, diuretic abuse, or over-exercise, but are unable to escape from the addiction by themselves. Anxiety, depression, and low self-esteem frequently coexist in these patients, often becoming their dominant thought and subsequently increasing the likelihood of co-morbidities like mood disorder and anxiety disorder (Carlos et al 2009). In contrast to patients with bulimia nervosa / binge eating disorder, those with restricting anorexia nervosa present obsessive eating habits less frequently (Emily et al 2008). They develop malnutrition, hormonal imbalances, and a variety of electrocardiographic abnormalities due to reduced total calorie intake and dehydration, which are the most lethal manifestations, and thus are important in the treatment of the patients.

Recently, we encountered a remarkable and uncommon case of an adolescent with restricting anorexia nervosa who presented with obsessive and restricted banana ingestion for more than 2 years (Tazoe et al 2007). As a result, the patient developed extreme hyperkalemia, hyperdopaminemia, pseudoaldosteronism, and dysthymia, which could not be explained by the pathology of restricting anorexia nervosa alone. Moreover, the patient had presented with obvious aggression and inner-impulse paralleling an increase in whole blood dopamine, suggesting that the brain dopamine concentration was also affected by the

obsessive and restricted banana ingestion. Since bananas are known to be rich sources of both dopamine and potassium (Kanazawa and Sakakibara, 2000; Kasuga A, 2008), the clinical condition of this patient was thought to be dramatically altered by the massive ingestion of bananas.

Case

At the age of 15, the female patient visited a pediatric clinic for emaciation, amenorrhea, and appetite loss, which had been noted by her school teacher. The patient had been on a strict diet intentionally for the past half year, and had lost 6.2 kg of weight (decreasing from 46.9 to 40.7 kg; BMI (body mass index) = 15.7). She was born at term, her psychomotor development was normal, and had no past history of Attention Deficit / Hyperactivity Disorder or other behavioral problems. Her pulse rate and blood pressure were within the normal range, and the electrocardiogram and cardiac ultrasound showed no abnormality. Although no abnormality was found in the regular blood analysis data, obvious hormonal imbalances were noted as follows:

GH (Growth hormone) 1.47 ng/ml (↓), IGF-1 (Insulin-like growth factor-1, somatomedin-C) 88 ng/ml (→), ACTH (Adrenocorticotropic hormone) 14 pg/ml (→), Free T4 0.81 ng/dl (↓), Free T3 1.65 pg/ml (↓), TSH (Thyroid stimulating hormone) 1.740 μU/l (→), and estradiol <10 pg/ml (↓). Minor elements such as Cu, Zn, vitamins B_1 and B_2, lactate, and pyruvate were all within normal ranges. She had pigmentation of the skin and was obviously hyperactive.

Obsessive Banana Ingestion Directly Affects the Blood Dopamine Concentration and Electrolytes

Figure 1 shows the course of illness observed in the patient. She was hospitalized two times over a 60-month observation period, and the lowest body weight reported was 27.0 kg (BMI = 10.3). An increase in extraordinarily obsessive behavior began to be observed during her first hospitalization period (from the 8th month of the observed period). She denied ingesting any food item other than bananas (5–20 pieces a day) and hard mineral water (up to 500 ml a day), and was obsessed by the need to engage in excessive daily exercise. Following this obsessive eating behavior, blood analysis showed a gradual increase of serum potassium and whole blood dopamine. The second hospitalization period was required when her body weight dropped as low as 27.0 kg at the 16th month of the observation period. Intravenous hyperalimentation along with cognitive-behavioral therapy was performed during each hospitalization period.

After the 24th month of the observation period, the patient's whole blood dopamine concentration jumped to 180 ng/ml. At the same time, her serum potassium was as high as 6.1 mEq/l, although no abnormality was observed in electrocardiogram and blood pressure examination. Later, in the 38th month of the observed period, her dopamine concentration increased to as high as 210 ng/ml. At the 40th month of the observation period, her weight decreased again to 32 kg. Her serum potassium level was 5.7 mEq/l, aldosterone was 708.8

ng/dl, and renin was 130 pg/ml, all of which are relatively higher than the normal range in the Japanese population. Although the patient kept normal blood pressure throughout the course of the illness, the increases in renin and aldosterone suggested that she fell into a state of pseudoaldosteronism during this period. Serum catecholamine analysis showed an extreme increase of free dopamine (0.47 ng/ml, normal range < 0.03); however, no increase in epinephrine (<0.01 ng/ml) or norepinephrine (0.39 ng/ml) was observed.

In response to treatment with cognitive-behavioral therapy, she began to ingest food items other than banana after 26 months of this restrictive eating pattern. Over the next 12 months, economic reasons prevented her from returning to the clinic; however, the most recent examination at the 56th month of the observation period showed distinct improvement in her blood values, including serum potassium of 5.6 mEq/l and whole blood dopamine of 56 ng/ml. In addition, her weight had increased to 36 kg. She seemed at that time to have "calmed down" and her skin was obviously depigmented.

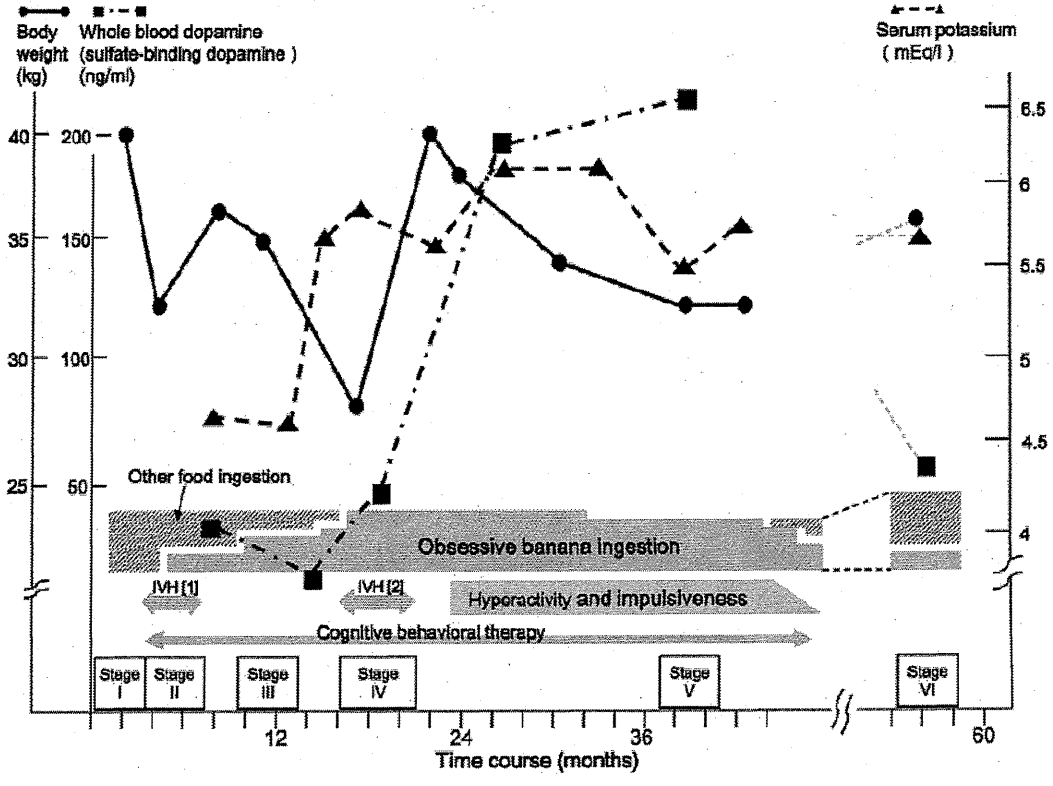

Figure 1. The course of illness in the patient with obsessive banana ingestion
The illness course of the patient is schematically presented. Changes in body weight, whole blood dopamine, serum potassium, and habit of food ingestion are shown. Two intravenous hyperalimentation treatments during hospitalization (IVH [1] and IVH [2]) and continuous cognitive-behavioral therapy were performed. The stages indicated in the figure correspond to the descriptions in the text.

OBSESSIVE BANANA INGESTION MAY HAVE MODIFIED THE PSYCHOBIOLOGICAL STATE IN THE PATIENT

The patient's psychological state had been continuously assessed by our team clinical psychologist (M.T.) regularly during the course of her illness, using three types of psychological tests: the tree drawing test (Koch, 1952; Kosaka, 2008), the Japanese version of the state-trait anxiety inventory (STAI) (Iwata et al 1998), and the Tokyo University egogram (TEG), which evaluates ego states (Oshima et al 1996).

The whole clinical course was classified to six stages according to the degree of emaciation, treatment, and blood analyses as follows (see also Figure 1).

Stage I. Prior to the first hospitalization: She did not cooperate with the psychological therapy or with oral ingestion of nutrient drinks. She walked more than 10 km daily, and exercised her abdominal muscles intensively to build her "ideal body." One drawing (Figure 2) was obtained during this stage.

Stage II. First admission: Within 6 months after the first visit, she had reduced her weight to 32.1 kg (BMI = 12.2). She underwent forced admission to the pediatric ward, where she was treated by intravenous hyperalimentation infusion, along with behavior restriction therapy. She gained 4 kg during the 30-day admission, and was discharged from the hospital afterward. Two drawings (Figures 3A and 3B) were obtained during this period.

Stage III. Between the first and second hospitalizations: The patient was obsessed by the idea that all processed foodstuffs are contaminated by additives and pesticides. Eventually, she stopped eating except for a maximum of 20 pieces of banana and 500 ml of mineral water per day. She stuck to one type of banana (an organic product from Ecuador) and one brand of hard mineral water. During this period, two drawings (Figures 4A and 4B) were obtained from the patient.

Stage IV. Second hospitalization: Her weight dropped to 27.0 kg (BMI = 10.3) at this time, which again became an indication for intravenous hyperalimentation treatment and admission. This time she gained over 13 kg and was discharged. However, there was no change in her eating and exercise habit. Two drawings (Figures 5A and 5B) were obtained during this period.

Stage V. Increase in blood dopamine level due to excessive consumption of bananas: Against the counsel of physicians, psychologists, and her family members, the patient continued her strict avoidance of food items other than bananas and hard mineral water. Blood analysis revealed increased levels of serum potassium, whole blood dopamine, aldosterone, renin, and angiotensin, which suggested a state of pseudo-aldosteronism and hyperdopaminemia. At this stage, she also began to show obvious impulsiveness and irritability, which are not frequently observed in anorexia nervosa patients. One drawing (Figure 6) was obtained during this period.

Stage VI. Remission from the obsessive banana ingestion with recovery of all of the blood values: Her impulsiveness and irritability had almost disappeared and she was eating many kinds of food, although the amount was still small. One drawing (Figure 7) was obtained during this period.